Letter

Plasmonic excitation for a tunable transmitter without magnetic field immune to backscattering

Aleksandr S. Petrov *

Laboratory of 2D Materials' Optoelectronics, Moscow Institute of Physics and Technology, 141701 Moscow, Russia

(Received 4 April 2021; revised 20 September 2021; accepted 10 December 2021; published 21 December 2021)

We predict a plasmonic excitation that exhibits chiral properties in the absence of external magnetic field. This excitation, that we call an interedge chiral Berry plasmon (IE CBP), is bound to an interface between two two-dimensional electron systems with different anomalous Hall conductivities. Crucially, the IE CBP is a unidirectional mode whose propagation direction and frequency are susceptible to external control, in sharp contrast to state-of-the-art magnetic field-free devices. We believe that the IE CBP represents a unique platform for tunable backscattering-immune signal transmission in the absence of magnetic field.

DOI: 10.1103/PhysRevB.104.L241407

I. INTRODUCTION

Nonreciprocal devices constitute a crucial part of modern technology. Nonreciprocal phenomena can only be manifested in systems with broken Lorentz reciprocity [1], which is conventionally achieved by external magnetic field bias. Expectantly, an extreme and highly desirable form of nonreciprocity, unidirectional transport, has long been possible at correspondingly utmost conditions: quantizing magnetic fields and helium temperatures [2] [the quantum Hall effect (QHE)]. Under such conditions, electrons propagate unidirectionally and without backscattering along the edges of a two-dimensional electron system (2DES), giving rise to a nonzero quantum Hall conductance. It was found that the quantum Hall conductance is closely connected with topology of electronic band structure through an integral of a band-defined quantity $\Omega(\mathbf{k})$ over the 2D crystal Brillouin zone (BZ):

$$\sigma_{xy} = \frac{e^2}{h}\mathcal{F}; \quad \mathcal{F} = \sum_i \int_{\mathrm{BZ}} d^2k\ \Omega(\mathbf{k}) f_i^0(\mathbf{k}), \tag{1}$$

where $e > 0$ is the elementary charge, h is the Planck constant, $f_i^0(\mathbf{k})$ is the equilibrium band occupancy (equal either to 1 or 0 in the QHE case), and the summation is performed over all the bands. The quantities $\Omega(\mathbf{k})$ and $\mathcal{F}$ are now known as the Berry curvature and the Berry flux, respectively [3,4]. In the QHE setup, $\mathcal{F}$ assumes integer values, referred to as Chern numbers [5,6].

Thus, the QHE takes place due to nonzero Berry flux of the 2D crystal Bloch bands modified by external magnetic field [7]. However, one can achieve $\mathcal{F} \neq 0$ even in the absence of magnetic bias in specially designed Bloch bands with broken time-reversal symmetry, as first proposed by Haldane [8]. His work provoked a burst of research interest and led to discovery of many profound phenomena, e.g., quantum spin Hall effect [9–11], topological insulation in three dimensions (3D) [12–15], or topological plasmonics [16–18]. Still, all these effects are very challenging to observe, as they require nanometer-precision production and low temperatures.

The situation drastically changes if we transfer the topological insight obtained for electronic bands in solid state to photonic bands in metastructures [19,20]. Thus, Wang *et al.* [21] demonstrated unidirectional, backscattering-immune signal transmission at room temperature in a magneto-optical photonic crystal. These works paved the way for the development of photonic topological insulators (PTIs) with many bright results obtained to date, see a recent review for details [22]. In general, PTIs seem to be a much more attractive platform than electronic systems: generally, PTIs require less technological precision ($\gtrsim 1\mu$m), operate at room temperature without magnetic field, and can even be made complementary metal-oxide semiconductor compatible [23].

Still, electronic systems hold a strong advantage over PTIs: their properties can be easily tuned. Indeed, condensed matter systems and particularly 2DESs benefit from numerous control techniques: field effect, external illumination, heating, etc. In turn, PTIs acquire their properties on the fabrication stage and further operate as is for scarce exceptions [24].

In this paper, we propose a concept of a unidirectional plasmonic transmitter that is both tunable and magnetic field free. The basic part of the transmitter represents a contact between two 2DESs with different Berry fluxes, as shown in Fig. 1. As we show below, the boundary between such 2DESs hosts a type of plasmonic modes that we call the *interedge chiral Berry plasmon* (IE CBP). This mode combines the properties of two previously known modes: (1) it arises due to an interplay between electron-electron interactions and finite Berry flux as a CBP [17,25,26], and (2) it is truly unidirectional as an interedge magnetoplasmon (IEMP) [27–32]. In what follows, we obtain the dispersion relation for the IE CBP and suggest a possible scheme of an IE CBP-based unidirectional transmitter.

II. THEORETICAL FORMALISM

The IE CBP dispersion relation can be obtained by modifying a known theory of the IEMP [28]. According to that work, in a local model of electron transport with spatially

* aleksandr.petrov@phystech.edu

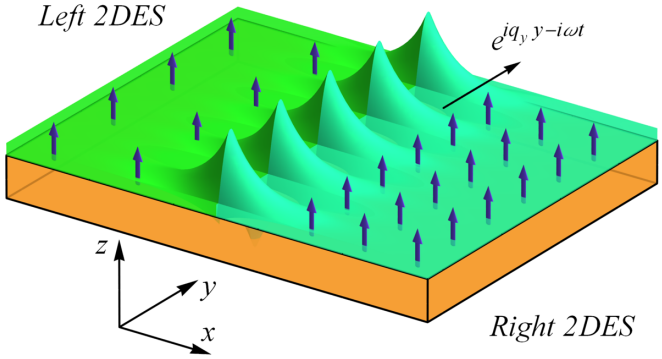

FIG. 1. Scheme of an interedge chiral Berry plasmon (IE CBP) bound to a contact between two two-dimensional electron systems (2DESs) with different Berry fluxes. The green and cyan areas denote the 2DESs, the orange area is the substrate, and the density of arrows stands for the Berry flux. The Berry flux is a vector $\mathcal{F}\hat{\mathbf{z}}$ that can be thought of as an intrinsic magnetic field and leads to nonzero anomalous Hall conductivity σ_{xy}. The off-diagonal conductivity contrast naturally induces the emergence of an interedge plasmonic mode.

homogeneous conductivities $\sigma_{xx}^{(r)}, \sigma_{xy}^{(r)}, \sigma_{xx}^{(l)}, \sigma_{xy}^{(l)}$, a boundary between the right (r) and left (l) 2DESs hosts an interedge plasmon mode (that is not necessarily magnetoplasmon), whose dispersion equation reads (eq. (28) in Ref. [28])

$$1 + \frac{q_y \Delta\sigma_{xy}}{i|q_y|\Delta\sigma_{xx}} \times \tanh\left\{\frac{1}{\pi}\int_0^\infty \frac{d\xi}{1+\xi^2} \ln\left[\frac{\varepsilon^{(r)}(q,\omega)}{\varepsilon^{(l)}(q,\omega)}\right]_{q_x=|q_y|\xi}\right\} = 0, \tag{2}$$

where $q_{x,y}$ are the wave vectors, $q = |\mathbf{q_x} + \mathbf{q_y}|$, $\varepsilon^{(r,l)}$ is plasma permittivity in the right (left) 2DES, $\Delta\chi = \chi^{(r)} - \chi^{(l)}$, where $\chi^{(r,l)}$ is any quantity related to the right (left) 2DES. The dispersion in Eq. (2) is solvable for any finite off-diagonal conductivity contrast $\Delta\sigma_{xy}$, regardless of its nature (but provided it is local). For example, the (inter)edge magnetoplasmon dispersion $\omega(q_y)$ is obtained by substituting the corresponding magnetic field-dependent conductivities into Eq. (2).

In our case, the off-diagonal conductivity is determined by Eq. (1), and its contrast arises due to the Berry flux contrast between the 2DESs. At the same time, the diagonal conductivity is not affected by the Berry flux [26,33]. Thus, we write $\Delta\sigma_{xy} = e^2\Delta\mathcal{F}/h$ and $\Delta\sigma_{xx} = ie^2\Delta n/m\omega$, then substitute these expressions into Eq. (2) and arrive at

$$\mathrm{sign}(q_y) = \frac{\omega}{\omega_\mathcal{F}} \tanh\left\{\frac{1}{\pi}\left[F\left(\frac{\omega_r^2}{\omega^2}\right) - F\left(\frac{\omega_l^2}{\omega^2}\right)\right]\right\}, \tag{3}$$

where $\mathrm{sign}(q_y) = q_y/|q_y|$ corresponds to the plasmon propagation direction, $\omega_{r,l}^2 = e^2 n_{r,l}|q_y|/2\varepsilon\varepsilon_0 m$ is the $2d$ plasmon frequency, ε is the substrate dielectric permittivity, ε_0 is the vacuum permittivity, m is the electron effective mass:

$$\omega_\mathcal{F} = \frac{h\Delta n}{m\Delta\mathcal{F}}, \tag{4}$$

and $F(z)$ is an integral function defined as

$$F(z) = \int_0^{\pi/2} \ln\left(1 - \frac{z}{\cos t}\right) dt. \tag{5}$$

Here, $F(z)$ is a complex-valued function, and $\mathrm{Im}\, F(z) = \pi^2/2$ remains constant for $z \geqslant 1$.

Equation (3) is the dispersion relation for the IE CBP. This equation can be solved only numerically, yet we can point out its several properties. First, the IE CBP branch $\omega(q)$ lies below the bulk plasmon branches $\omega_{r,l}(q)$, or else it is subject to decay into the bulk (mathematically, this situation arises because the difference $F(\omega_r^2/\omega^2) - F(\omega_l^2/\omega^2)$ becomes complex valued at $\omega > \omega_{r,l}$). Next, the mode is unidirectional [34], as the propagation direction explicitly enters the dispersion equation and is determined by the Berry flux contrast: $\mathrm{sign}(q_y) = \mathrm{sign}(\Delta\mathcal{F})$. Finally, the IE CBP frequency is bound to a frequency window: its upper limit can be obtained in the short-wavelength limit:

$$\omega \to \omega_{\max} = \frac{h(n_r + n_l)}{m\Delta\mathcal{F}}\mathrm{sign}(q_y), \quad \omega_{r,l} \gg \omega_\mathcal{F}, \tag{6}$$

whereas its lower limit is determined by the lowest bulk frequency; if $\omega_r > \omega_l$, we substitute $\omega_{\min} = \omega_l(q_{\mathrm{th}})$ into Eq. (3) and obtain

$$\omega_{\min} = \frac{\omega_\mathcal{F}\ \mathrm{sign}(q_y)}{\tanh\left\{\frac{1}{\pi}\left[F\left(\frac{n_r}{n_l}\right) - F(1)\right]\right\}}, \tag{7}$$

where q_{th} is the threshold wave vector below which the IE CBP does not exist. We note that $\omega_{\max} > \omega_{\min}$ for all carrier densities; for ordinary materials with $\sigma_{xy}^{AH} = 0$, both $\omega_{\min}$ and $\omega_{\max}$ tend to infinity, which corresponds to the absence of IE CBP in such materials.

III. DISCUSSION

A. Distinction between IE CBP, IEMP, and CBP

Having described basic properties of the IE CBP, we now point out its similarities and differences from the predecessors, CBP and IEMP.

First, the IE CBP can be regarded as an extended version of a CBP where the vacuum (transparent system) near the edge of a 2DES is replaced with another 2DES (opaque system). This seemingly minor distinction leads to a fundamentally different behavior of unidirectional modes: while in the CBP setup, there does exist a backward-propagating mode that just merges with the continuum at a certain wave vector, the IE CBP case precludes the existence of such a mode. In this sense, edge plasmons seem to be analogous to surface plasmons, where truly one-way modes have recently been shown to exist only on opaque-opaque boundaries due to topological protection [32,35,36].

From the other hand, the IE CBP can also be seen as the anomalous Hall version of the IEMP. However, in the IEMP case, the applied magnetic field impacts both diagonal and off-diagonal conductivities, making the latter frequency dependent. In contrast, the IE CBP diagonal conductivity is unaffected by the Berry flux, while the off-diagonal conductivity is independent of frequency or collisional damping. These conductivity features lead to functionally different dispersion curves for IEMP and IE CBP despite a similar ansatz

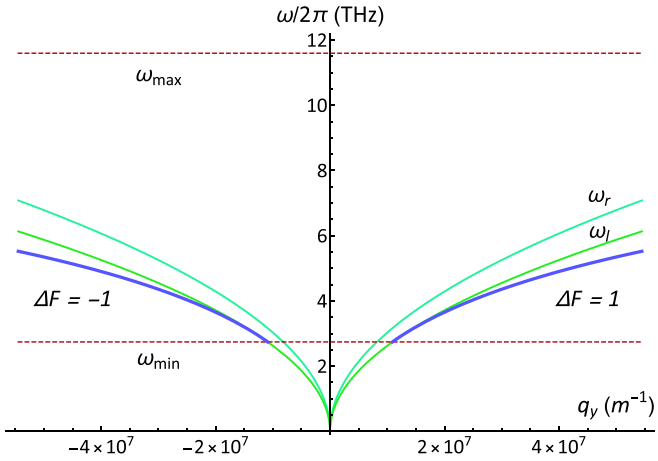

FIG. 2. Dispersion curves for plasmon modes in bilayer graphene on SiO_2 substrate in the configuration of Fig. 1 and parameters given in the main text. The interedge chiral Berry plasmon (IE CBP; blue lines) is a gapped excitation that is bound to a frequency region between $\omega_{\min}$ and $\omega_{\max}$ (dashed lines) given by Eqs. (6) and (7). The IE CBP propagation direction is determined by the sign of $\Delta\mathcal{F}$. The bulk plasmon dispersion is unaffected by the Berry flux and is shown by green and cyan lines.

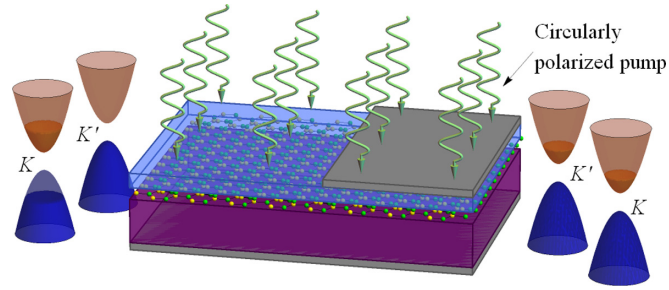

FIG. 3. Schematic view of a device for interedge chiral Berry plasmon (IE CBP) observation in bilayer graphene (BLG). The gate electrodes are shown in gray; purple and light blue areas correspond to dielectric media; curvy arrows denote circularly polarized pump; and paraboloids beside the structure stand for BLG valleys. The left part of BLG is valley polarized and possesses nonzero Berry flux, whereas the right part of BLG is shaded by the top gate and rests in equilibrium. The boundary between the left and right BLG parts supports the IE CBP whose properties can be tuned by the two gate voltages as well as by pump polarization and intensity.

[see Eq. (2)], the most prominent difference is gap opening in the IE CBP case.

B. Materials consideration

IE CBPs can be observed in a range of materials that exhibit anomalous Hall effect (AHE). For example, finite $\mathcal{F}$ is known to arise in magnetically ordered semiconductors, such as Bi_2Te_3 [37,38], HgTe quantum wells [39], or InAs/GaSb [40], or in nonequilibrium gapped Dirac materials, e.g., graphene [25,41–43] or MoS_2 [44,45] pumped by circularly polarized light. For quantitative estimates, we choose biased bilayer graphene (BLG) on Si/SiO_2 substrate. In this case, we assume $m = 0.035m_e$, $\varepsilon = (4+1)/2 = 2.5$, $n_r = 2\times10^{11}\,\mathrm{cm}^{-2}$, $n_l = 1.5\times10^{11}\,\mathrm{cm}^{-2}$, and the Berry flux can reach $\Delta\mathcal{F} = 1$ [25]. With these values, we solve Eq. (3) numerically and plot the dispersion $\omega(q)$ in Fig. 2. We observe all the aforementioned features: gapped spectrum, unidirectionality determined by $\mathrm{sign}(\Delta\mathcal{F})$, bound spectrum with the borders given by Eqs. (6) and (7). We note that the $\omega_{\max}$ value usually lies much higher than experimentally relevant frequencies; in Fig. 2, it seems to have no effect on the IE CBP, yet we checked that it is indeed the upper asymptote for the $\omega_{\mathrm{IE\,CBP}}$ curve (if we extrapolate the curve to unphysically large wave vectors). The IE CBP frequency lies in the terahertz range and corresponds to wavelengths on the order of 0.1–1 μm.

The realization of IE CBP in BLG can be achieved in a device schematically shown in Fig. 3: a BLG structure is exposed to circularly polarized light that selectively excites carriers in one of the BLG valleys [25,43]. However, a part of the sample is covered by a top gate and rests in equilibrium. Notably, the top gate not only assists the nonuniform pump but also allows us to independently alter the carrier density in the corresponding part of the sample. Thus, we achieve full control over the IE CBP mode: we can change its propagation direction by the polarization of the pump beam as well as frequency by adjusting carrier densities by back and top gates and the pump intensity.

Our analysis corresponded to clean systems. The inevitable loss mechanisms are usually described by effective plasmon lifetime τ that can reach values on the order of 10 ps in cutting edge graphene plasmonic experiments [46,47]. Thus, we can estimate the IE CBP propagation length as $l_{\mathrm{prop}} \simeq v_{\mathrm{gr}}\tau \simeq 10\,\mu$m, where $v_{\mathrm{gr}} = d\omega/dq \simeq 10^6$ m/s is the group velocity extracted from Fig. 2. While the estimated propagation length incorporates all graphene-associated damping mechanisms, the substrate losses should still be considered, which lowers plasmon propagation length to several microns [47,48].

However, not all the platforms promise long plasmon propagation lengths. For instance, magnetically doped semiconductors can hardly be considered plasmonic materials due to high residual resistivity that results into relaxation times 10–100 fs even at millikelvin temperatures [17,37,49] and plasmon propagation lengths not longer than 100 nm. However, this estimate shifts by orders of magnitude if we push our system into the QAH regime when electrons travel along edge channels with hardly any scattering. In this case, the effective relaxation time is no longer determined by the bulk mobility and allows for plasmon propagation over hundreds of microns, as shown in recent experiments [17]. Undoubtedly, the model system depicted in Fig. 1 supports interedge modes in the QAH case, but it is unclear whether the developed classical theory is applicable in this regime. It should be noted, however, that plasmons in the ordinary quantum Hall regime are well described by classical theories [50–53], and we may speculate that the same holds for the QAH case. The rigorous description of IE CBP in the QAH regime is a matter for separate research, though.

We stress that the number of techniques that enable AHE in high-mobility samples constantly grows. Thus, in recent years, such observations as proximity-induced ferromagnetism [54,55] (which precludes dopant-induced residual

resistance), AHE in nonmagnetic 2DES [56], or even AHE in artificially corrugated BLG [57] were reported.

IV. CONCLUSIONS

In conclusion, we presented the theory of a terahertz plasmonic excitation, the IE CBP, that exhibits unidirectional propagation in the absence of magnetic field. Its frequency lies in the terahertz range and can be tuned externally as well as the propagation direction, in distinction from the state-of-the-art metamaterial-based unidirectional transmitters. We also suggested a BLG-based device scheme where IE CBP propagation length can reach 10 μm and discussed other promising material platforms. Thus, the IE CBP can serve for future tunable magnetic field-free unidirectional transmitters in the far-infrared part of the spectrum.

ACKNOWLEDGMENTS

The author is indebted to Dmitry Svintsov for profound guidance and support; he is also grateful to D. Bandurin for stimulating discussions. This paper was supported by the Foundation for the Advancement of Theoretical Physics and Mathematics BASIS, Project No. 18-1-5-66-1 and by the Russian Presidential Scholarship SP-429.2021.5. The development of the BLG device scheme was conducted in the framework of the Russian Foundation for Basic Research, Project No. 18-29-20116.

[1] D. Jalas, A. Petrov, M. Eich, W. Freude, S. Fan, Z. Yu, R. Baets, M. Popović, A. Melloni, J. D. Joannopoulos *et al.*, What is-and what is not-an optical isolator, Nat. Photonics **7**, 579 (2013).

[2] K. v. Klitzing, G. Dorda, and M. Pepper, New Method for High-Accuracy Determination of the Fine-Structure Constant Based on Quantized Hall Resistance, Phys. Rev. Lett. **45**, 494 (1980).

[3] M. V. Berry, Quantal phase factors accompanying adiabatic changes, Proc. R. Soc. Lond. A **392**, 45 (1984).

[4] D. Xiao, M.-C. Chang, and Q. Niu, Berry phase effects on electronic properties, Rev. Mod. Phys. **82**, 1959 (2010).

[5] R. B. Laughlin, Quantized Hall conductivity in two dimensions, Phys. Rev. B **23**, 5632 (1981).

[6] D. J. Thouless, M. Kohmoto, M. P. Nightingale, and M. den Nijs, Quantized Hall Conductance in a Two-Dimensional Periodic Potential, Phys. Rev. Lett. **49**, 405 (1982).

[7] D. R. Hofstadter, Energy levels and wave functions of Bloch electrons in rational and irrational magnetic fields, Phys. Rev. B **14**, 2239 (1976).

[8] F. D. M. Haldane, Model for a Quantum Hall Effect without Landau Levels: Condensed-Matter Realization of the "Parity Anomaly", Phys. Rev. Lett. **61**, 2015 (1988).

[9] C. L. Kane and E. J. Mele, Quantum Spin Hall Effect in Graphene, Phys. Rev. Lett. **95**, 226801 (2005).

[10] B. A. Bernevig, T. L. Hughes, and S.-C. Zhang, Quantum spin Hall effect and topological phase transition in HgTe quantum wells, Science **314**, 1757 (2006).

[11] M. König, S. Wiedmann, C. Brüne, A. Roth, H. Buhmann, L. W. Molenkamp, X.-L. Qi, and S.-C. Zhang, Quantum spin Hall insulator state in HgTe quantum wells, Science **318**, 766 (2007).

[12] R. Roy, Topological phases and the quantum spin Hall effect in three dimensions, Phys. Rev. B **79**, 195322 (2009).

[13] L. Fu, C. L. Kane, and E. J. Mele, Topological Insulators in Three Dimensions, Phys. Rev. Lett. **98**, 106803 (2007).

[14] J. E. Moore and L. Balents, Topological invariants of time-reversal-invariant band structures, Phys. Rev. B **75**, 121306(R) (2007).

[15] Y. Chen, J. G. Analytis, J.-H. Chu, Z. Liu, S.-K. Mo, X.-L. Qi, H. Zhang, D. Lu, X. Dai, Z. Fang *et al.*, Experimental realization of a three-dimensional topological insulator, Bi_2Te_3, Science **325**, 178 (2009).

[16] P. Di Pietro, M. Ortolani, O. Limaj, A. Di Gaspare, V. Giliberti, F. Giorgianni, M. Brahlek, N. Bansal, N. Koirala, S. Oh *et al.*, Observation of Dirac plasmons in a topological insulator, Nat. Nanotechnol. **8**, 556 (2013).

[17] A. C. Mahoney, J. I. Colless, L. Peeters, S. J. Pauka, E. J. Fox, X. Kou, L. Pan, K. L. Wang, D. Goldhaber-Gordon, and D. J. Reilly, Zero-field edge plasmons in a magnetic topological insulator, Nat. Commun. **8**, 1836 (2017).

[18] Y. Dai, Z. Zhou, A. Ghosh, R. S. Mong, A. Kubo, C.-B. Huang, and H. Petek, Plasmonic topological quasiparticle on the nanometre and femtosecond scales, Nature (London) **588**, 616 (2020).

[19] F. D. M. Haldane and S. Raghu, Possible Realization of Directional Optical Waveguides in Photonic Crystals with Broken Time-Reversal Symmetry, Phys. Rev. Lett. **100**, 013904 (2008).

[20] S. Raghu and F. D. M. Haldane, Analogs of quantum-hall-effect edge states in photonic crystals, Phys. Rev. A **78**, 033834 (2008).

[21] Z. Wang, Y. Chong, J. D. Joannopoulos, and M. Soljačić, Observation of unidirectional backscattering-immune topological electromagnetic states, Nature (London) **461**, 772 (2009).

[22] T. Ozawa, H. M. Price, A. Amo, N. Goldman, M. Hafezi, L. Lu, M. C. Rechtsman, D. Schuster, J. Simon, O. Zilberberg, and I. Carusotto, Topological photonics, Rev. Mod. Phys. **91**, 015006 (2019).

[23] Y. Yang, Y. Yamagami, X. Yu, P. Pitchappa, J. Webber, B. Zhang, M. Fujita, T. Nagatsuma, and R. Singh, Terahertz topological photonics for on-chip communication, Nat. Photonics **14**, 446 (2020).

[24] X. Cheng, C. Jouvaud, X. Ni, S. H. Mousavi, A. Z. Genack, and A. B. Khanikaev, Robust reconfigurable electromagnetic pathways within a photonic topological insulator, Nat. Mater. **15**, 542 (2016).

[25] A. Kumar, A. Nemilentsau, K. H. Fung, G. Hanson, N. X. Fang, and T. Low, Chiral plasmon in gapped Dirac systems, Phys. Rev. B **93**, 041413(R) (2016).

[26] J. C. Song and M. S. Rudner, Chiral plasmons without magnetic field, Proc. Natl. Acad. Sci. **113**, 4658 (2016).

[27] A. L. Fetter, Edge magnetoplasmons in a bounded two-dimensional electron fluid, Phys. Rev. B **32**, 7676 (1985).

[28] V. Volkov and S. A. Mikhailov, Edge magnetoplasmons: low frequency weakly damped excitations in inhomogeneous two-dimensional electron systems, ZhETF **94**, 217 (1988) [Sov. Phys. JETP **67**, 1639 (1988)].

[29] S. A. Mikhailov and V. Volkov, Inter-edge magnetoplasmons in inhomogeneous two-dimensional electron systems, J. Phys.: Condens. Matter **4**, 6523 (1992).

[30] A. S. Petrov and D. Svintsov, Thresholdless excitation of edge plasmons by transverse current, Phys. Rev. B **102**, 121402(R) (2020).

[31] D. Jin, L. Lu, Z. Wang, C. Fang, J. D. Joannopoulos, M. Soljačić, L. Fu, and N. X. Fang, Topological magnetoplasmon, Nat. Commun. **7**, 13486 (2016).

[32] F. Monticone, A truly one-way lane for surface plasmon polaritons, Nat. Photonics **14**, 461 (2020).

[33] A. S. Petrov and D. Svintsov, Perturbation theory for two-dimensional hydrodynamic plasmons, Phys. Rev. B **99**, 195437 (2019).

[34] Unidirectionality should not be confused with the absence of backscattering, e.g., backscattering-immune plasmons were predicted to exist in graphene nanoribbons [58], yet these plasmons are not unidirectional: there still exists a backward-propagating mode that is just uncoupled from the forward-propagating mode. In contrast, IE CBP does not allow for backward propagation in principle.

[35] M. G. Silveirinha, Chern invariants for continuous media, Phys. Rev. B **92**, 125153 (2015).

[36] S. A. H. Gangaraj and F. Monticone, Do truly unidirectional surface plasmon-polaritons exist? Optica **6**, 1158 (2019).

[37] C.-Z. Chang, J. Zhang, X. Feng, J. Shen, Z. Zhang, M. Guo, K. Li, Y. Ou, P. Wei, L.-L. Wang *et al.*, Experimental observation of the quantum anomalous Hall effect in a magnetic topological insulator, Science **340**, 167 (2013).

[38] Y. Deng, Y. Yu, M. Z. Shi, Z. Guo, Z. Xu, J. Wang, X. H. Chen, and Y. Zhang, Quantum anomalous Hall effect in intrinsic magnetic topological insulator $MnBi_2Te_4$, Science **367**, 895 (2020).

[39] C.-X. Liu, X.-L. Qi, X. Dai, Z. Fang, and S.-C. Zhang, Quantum Anomalous Hall Effect in $Hg_{1-y}Mn_yTe$ Quantum Wells, Phys. Rev. Lett. **101**, 146802 (2008).

[40] Q.-Z. Wang, X. Liu, H.-J. Zhang, N. Samarth, S.-C. Zhang, and C.-X. Liu, Quantum Anomalous Hall Effect in Magnetically Doped InAs/GaSb Quantum Wells, Phys. Rev. Lett. **113**, 147201 (2014).

[41] T. Oka and H. Aoki, Photovoltaic Hall effect in graphene, Phys. Rev. B **79**, 081406(R) (2009).

[42] J. W. McIver, B. Schulte, F.-U. Stein, T. Matsuyama, G. Jotzu, G. Meier, and A. Cavalleri, Light-induced anomalous Hall effect in graphene, Nat. Phys. **16**, 38 (2020).

[43] A. Friedlan and M. M. Dignam, Valley polarization in biased bilayer graphene using circularly polarized light, Phys. Rev. B **103**, 075414 (2021).

[44] K. F. Mak, K. L. McGill, J. Park, and P. L. McEuen, The valley Hall effect in MoS_2 transistors, Science **344**, 1489 (2014).

[45] Y. Peng, J. Chen, Y. Song, and Y. Li, Characterization of photo-induced anomalous Hall effect in the two-dimensional MoS_2, Appl. Surf. Sci. **366**, 310 (2016).

[46] L. Wang, I. Meric, P. Huang, Q. Gao, Y. Gao, H. Tran, T. Taniguchi, K. Watanabe, L. Campos, D. Muller *et al.*, One-dimensional electrical contact to a two-dimensional material, Science **342**, 614 (2013).

[47] G. X. Ni, A. S. McLeod, Z. Sun, L. Wang, L. Xiong, K. W. Post, S. S. Sunku, B.-Y. Jiang, J. Hone, C. R. Dean *et al.*, Fundamental limits to graphene plasmonics, Nature (London) **557**, 530 (2018).

[48] D. A. Bandurin, D. Svintsov, I. Gayduchenko, S. G. Xu, A. Principi, M. Moskotin, I. Tretyakov, D. Yagodkin, S. Zhukov, T. Taniguchi *et al.*, Resonant terahertz detection using graphene plasmons, Nat. Commun. **9**, 1 (2018).

[49] L. Du, I. Knez, G. Sullivan, and R.-R. Du, Robust Helical Edge Transport in Gated InAs/GaSb Bilayers, Phys. Rev. Lett. **114**, 096802 (2015).

[50] D. B. Chklovskii, B. I. Shklovskii, and L. I. Glazman, Electrostatics of edge channels, Phys. Rev. B **46**, 4026 (1992).

[51] I. L. Aleiner and L. I. Glazman, Novel Edge Excitations of Two-Dimensional Electron Liquid in a Magnetic Field, Phys. Rev. Lett. **72**, 2935 (1994).

[52] M. D. Johnson and G. Vignale, Dynamics of dissipative quantum Hall edges, Phys. Rev. B **67**, 205332 (2003).

[53] S. Bosco and D. P. DiVincenzo, Nonreciprocal quantum Hall devices with driven edge magnetoplasmons in two-dimensional materials, Phys. Rev. B **95**, 195317 (2017).

[54] Z. Wang, C. Tang, R. Sachs, Y. Barlas, and J. Shi, Proximity-Induced Ferromagnetism in Graphene Revealed by the Anomalous Hall Effect, Phys. Rev. Lett. **114**, 016603 (2015).

[55] H.-D. Song, P.-F. Zhu, J. Fang, Z. Zhou, H. Yang, K. Wang, J. Li, D. Yu, Z. Wei, and Z.-M. Liao, Anomalous Hall effect in graphene coupled to a layered magnetic semiconductor, Phys. Rev. B **103**, 125304 (2021).

[56] D. Maryenko, A. Mishchenko, M. Bahramy, A. Ernst, J. Falson, Y. Kozuka, A. Tsukazaki, N. Nagaosa, and M. Kawasaki, Observation of anomalous Hall effect in a non-magnetic two-dimensional electron system, Nat. Commun. **8**, 14777 (2017).

[57] S.-C. Ho, C.-H. Chang, Y.-C. Hsieh, S.-T. Lo, B. Huang, T.-H.-Y. Vu, C. Ortix, and T.-M. Chen, Hall effects in artificially corrugated bilayer graphene without breaking time-reversal symmetry, Nature Electronics **4**, 116 (2021).

[58] L. Brey and H. A. Fertig, Elementary electronic excitations in graphene nanoribbons, Phys. Rev. B **75**, 125434 (2007).